Direct Torque Control of Permanent Magnet Brushless AC Drive with Single-Phase Open-Circuit Fault Accounting for Influence of Inverter Voltage Drop

K. D. Hoang Z.Q. Zhu M. P. Foster
Department of Electronic and Electrical Engineering, The University of Sheffield, Sheffield, United Kingdom
Email: k.hoang@sheffield.ac.uk

Abstract: This paper presents a novel direct torque control (DTC) of permanent magnet (PM) brushless AC (BLAC) drive under single-phase open-circuit fault (SOF) accounting for the influences of inverter voltage drop, together with novel current model-based and voltage model-based stator flux estimation schemes for post-fault operation. It is demonstrated that for accurately elaborating the modified mathematical model, the voltage induced in the stator open phase winding and its relevant flux linkage should be taken into account although they do not contribute to torque production in the post-fault operating mode. It is also proven that reconfiguration of the conventional six-switch three-phase inverter for the purpose of fault-tolerant control results in a significant magnitude imbalance between the α- and β-components of inverter voltage drop (IVD). Thus, the influences of this unbalanced issue on performance of the two proposed stator flux estimation methods are investigated in details and a compensation method for the voltage model-based stator flux estimator is proposed and experimentally verified. It is shown that fault-tolerant control with high performance operation can be maintained for a DTC-based PM BLAC drive under SOF using the proposed modified mathematical model.

Abbreviations

AC	Alternating current
BLAC	Brushless AC
DC	Direct current
DTC	Direct torque control
ELES	Extra-leg extra-switch
EMF	Electromotive force
IPM	Interior PM
ITC	Indirect torque control
IVD	Inverter voltage drop
LPF	Low-pass filter
PM	Permanent magnet
SOF	Single-phase open-circuit fault
SPM	Surface-mounted PM
SSTP	Six-switch three phase

1. Introduction

Due to many advantageous characteristics, PM BLAC machines play an important role in industrial applications [1]. Normally, a six-switch three phase (SSTP) inverter [Fig. 1(a)] together with indirect torque control (ITC) [1], [2] or direct torque control (DTC) [3] techniques is often employed for a PM BLAC drive to achieve high performance operation. However, the SSTP scheme cannot satisfy the requirement of high reliability and fault tolerance, which is often the highest consideration for some safety-critical applications such as aerospace or automotive industry. A typical requirement of fault-tolerant capability would be keeping on driving a machine having single-phase open-circuit fault (SOF).

In [4] and [5], two inverter topologies utilizing DC bus midpoint connection to maintain the performance of an induction machine drive under SOF were proposed. However, value of the space voltage vector under these two schemes is reduced to half of that in the normal case [6] and therefore the maximum achievable speed is decreased to half of the nominal rating. On the other hand, due to the limited values of DC link capacitors, current waveforms may be seriously distorted at low-speed operation [7]. Another inverter topology termed as extra-leg extra-switch (ELES) scheme [Fig. 1(b)] where the neutral point is controlled via an extra inverter leg in the post-fault operation region was respectively adopted for induction machine drive [8] and interior PM (IPM) BLAC drive [9], [10] having SOF. Under this scheme, value of the space voltage vector is similar to that in the healthy condition [10] and therefore, maximum achievable speed is the same for both the healthy and post-fault cases. As electromagnetic torque of the machine controlled by this scheme is only contributed by the two remaining stator phases, a 60 electrical degree phase shift between the two remaining stator phase current waveforms is required to avoid torque ripples and an increase by $\sqrt{3}$ times compared to the pre-fault value in the current magnitude is demanded to maintain the same load torque [10]. Also from [9] and [10], it was demonstrated that in the post-fault operation region with space vector modulation technique, effects of the voltage induced in the stator open phase winding should be compensated by a feed-forward action to achieve constant dq-axis currents and smooth torque. Another torque ripple feed-forward compensation technique using zero sequence voltage was suggested in [11] and [12] for fault-tolerant control of matrix converter PM BLAC drive having SOF. However, it was proposed in [13] that this induced voltage should be set to zero for accurately modifying the mathematical model of an IPM BLAC machine under SOF fed by an ELES inverter using sine-triangle pulse width modulation technique. On the other hand, it was shown that

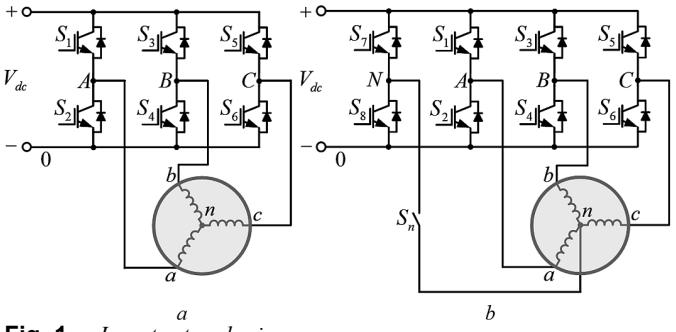

a b

Fig. 1 *Inverter topologies*
a SSTP scheme
b ELES scheme

for fault-tolerant control of a PM BLAC drive having SOF under hysteresis current control technique [14], this induced voltage should be neglected since only the information of the two remaining stator phase currents is required for the proposed control method.

In a DTC-based drive system, the stator flux linkage and electromagnetic torque are simultaneously controlled in the stationary ($\alpha\beta$) reference frame to achieve high performance operation [3], [15]. Thus, for post-fault performance of a DTC-based PM BLAC drive with SOF, mathematical model of the machine in the ($\alpha\beta$) reference frame must be modified to accurately estimate the stator flux linkage and the electromagnetic torque in the post-fault operating mode. In [16], it was shown that the stator flux associated with the induced voltage in the stator open phase winding is essential for application of DTC strategy to an ELES inverter PM BLAC drive under SOF. However, implementation of the stator flux linkage estimation scheme under this proposed DTC method requires a large amount of machine parameter information (phase voltages, phase currents, stator resistance, stator phase mutual inductance, PM flux linkage, rotor position). Normally, flux estimation strategies are categorized into two main models - current model where only the information of stator inductance, PM flux linkage, phase currents, and rotor position is required and voltage model where only the information of phase voltages, phase currents, and stator resistance is employed [15]. Also in [16], although simulation study of the proposed DTC achieved sinusoidal current waveforms, measured results of the tested PM BLAC machine with perfect sinusoidal back-electromotive forces (EMF) showed significant distorted current waveforms for which unbalanced phase back-EMFs and low-pass filter (LPF) effects were suggested to be accounted. In this paper, further study of the current distortion issue in the DTC-based ELES inverter PM BLAC drive having SOF together with the proposed remedy will be introduced.

In this paper, it is demonstrated that by simply modifying the conventional Clarke transformation for the two remaining stator phase currents in the post-fault operation region, the mathematical model of PM BLAC machine having SOF in the ($\alpha\beta$) reference frame can be achieved with novel current model-based and voltage model-based stator flux estimation schemes. Thus, it is proven that for accurately elaborating the modified mathematical model, the voltage induced in the stator open phase winding and its relevant stator flux linkage should be taken into account although they do not contribute to torque production in the post-fault operating mode. The novelty of the proposed mathematical model compared with the previous study [16] is the implementation of the proposed current model-based and voltage model-based stator flux estimators requires similar machine parameter information as that in the healthy case [15] except that the leakage inductance is additionally demanded for the proposed voltage model-based stator flux estimator. Thus, the proposed voltage model-based stator flux estimation scheme does not rely on the rotor position information. It is also shown that the reconfiguration from the SSTP scheme to the ELES scheme for fault-tolerant control purpose results in a significant magnitude imbalance between the α- and β-inverter voltage drop (IVD) components. Although this imbalanced issue does not adversely affect the performance of the proposed current model-based DTC, conventionally neglecting the IVD in the proposed voltage model-based estimator does lead to a significant magnitude imbalance between the α- and β-components of the estimated stator flux linkages. As a result, phase currents under the proposed voltage model-based DTC become seriously distorted. To solve this problem, a compensation scheme is proposed and verified by experimental results.

This paper is organized as follows. In Section 2, a modified mathematical model of a PM BLAC machine having SOF in the ($\alpha\beta$) reference frame is systematically analysed and presented. The application of DTC methodology to an ELES inverter PM BLAC drive with SOF using the proposed current model-based and voltage model-based stator flux estimators is respectively introduced in Section 3. In Section 4, imbalanced issue between the estimated α- and β-stator flux linkage components under the proposed voltage model-based stator flux estimator due to conventionally neglecting the inverter voltage drop (IVD) of the ELES inverter is demonstrated and an IVD compensation strategy is suggested. Then, measured results of the proposed voltage model-based and current model-based stator flux estimators under both ITC [14] and DTC are presented to verify the suggested stator flux estimation schemes. Simulation and experimental results are reported in Section 5 to validate the proposed DTC methodologies.

2. Modified mathematical model of a PM BLAC machine having SOF

To limit the scope, the paper is only focused on 3-phase surface-mounted PM (SPM) BLAC machine. The well-known mathematical model of a three-phase SPM BLAC machine in the stationary (*abc*) reference frame [17], [18] can be expressed as

$$v_{abcn} = Ri_{abc} + \frac{d\psi_{sabc}}{dt} \tag{1}$$

where $v_{abcn} = [v_{an} \quad v_{bn} \quad v_{cn}]^T$; $R = diag(R_s, R_s, R_s)$; $v_{an,bn,cn}$ and R_s are the stator phase-to-neutral voltages and the stator phase resistance, respectively; $i_{abc} = [i_a \quad i_b \quad i_c]^T$; $i_{a,b,c}$ are the stator phase currents.

$$\psi_{sabc} = Li_{abc} + \psi_{rabc} \tag{2}$$

where $\psi_{sabc} = [\psi_{sa} \quad \psi_{sb} \quad \psi_{sc}]^T$; $L = \begin{bmatrix} L_a & M_{ab} & M_{ac} \\ M_{ba} & L_b & M_{bc} \\ M_{ca} & M_{cb} & L_c \end{bmatrix}$;

$\psi_{rabc} = \psi_m[\cos(\theta_e) \quad \cos(\theta_e - \frac{2\pi}{3}) \quad \cos(\theta_e - \frac{4\pi}{3})]^T$; $\psi_{sa,sb,sc}$ are the stator fluxes; $L_{a,b,c}$ and $M_{ab,ac,ba,bc,ca,cb}$ are the stator phase self inductances and the stator phase mutual inductances; ψ_m is the PM flux linkage; θ_e is the electrical rotor position, respectively.

According to [18], stator winding inductances of a SPM BLAC machine can be defined as

$$L_{a,b,c} = L_{ls} + L_m \,;\, M_{ab,ba,ac,ca,bc,cb} = -\frac{L_m}{2} \,;\, L_s = L_{ls} + \frac{3L_m}{2} \tag{3}$$

where L_{ls}, L_m, and L_s is the stator phase leakage inductance, the stator phase magnetizing inductance, and the stator inductance, respectively.

$$T_e = p\left(i_{abc}^T \frac{d\psi_{rabc}}{d\theta_e}\right) \tag{4}$$

where T_e is the electromagnetic torque and p is the number of pole pairs.

When SOF occurs, assuming phase *a* is the open phase and therefore $i_a = 0$. Thus, to convert the two remaining stator phase currents from the (*abc*) reference frame to the (*αβ*) reference frame, the conventional Clarke transformation [18] can be modified as

$$\begin{bmatrix} i_\alpha \\ i_\beta \end{bmatrix} = K \begin{bmatrix} 1 & -\frac{1}{2} & -\frac{1}{2} \\ 0 & \frac{\sqrt{3}}{2} & -\frac{\sqrt{3}}{2} \end{bmatrix} \begin{bmatrix} 0 \\ i_b \\ i_c \end{bmatrix} \tag{5}$$

where the factor $K = 2/\sqrt{3}$ is chosen for magnitude invariant conversion [14] (see Appendix).

On the other hand, it is evident that in the post-fault operating mode, back-EMF is still induced in the stator open phase winding from the permanent magnet located in the spinning rotor [9], [10]. This induced back-EMF, together with the mutual voltages caused by the two remaining stator phase currents due to the effects of mutual inductances, form an induced voltage in the stator open phase winding. Therefore, the equations of the stator flux linkage and the stator phase voltage of a three-phase SPM BLAC machine having SOF in the (*abc*) reference frame still contain three individual components representing for three stator phases as that in the healthy case (1)-(2), but value of the stator open phase current is set as zero. Thus, to transfer these variables from the (*abc*) reference frame to the (*αβ*) reference frame, the conventional Clarke transformation [18] is utilized.

$$\begin{bmatrix} f_\alpha \\ f_\beta \end{bmatrix} = \frac{2}{3} \begin{bmatrix} 1 & -\frac{1}{2} & -\frac{1}{2} \\ 0 & \frac{\sqrt{3}}{2} & -\frac{\sqrt{3}}{2} \end{bmatrix} \begin{bmatrix} f_a \\ f_b \\ f_c \end{bmatrix} \tag{6}$$

where f is a dummy variable representing a stator phase voltage or flux linkage and the factor 2/3 is chosen for magnitude invariant conversion. By substituting (5) and (6) into (1), (2), (3), (4), the modified mathematical model of a SPM BLAC machine having SOF in the (*αβ*) reference frame can be derived.

$$v_\alpha = R_s \frac{i_\alpha}{\sqrt{3}} + \frac{d\psi_{s\alpha}}{dt} \tag{7}$$

$$v_\beta = R_s \frac{i_\beta}{\sqrt{3}} + \frac{d\psi_{s\beta}}{dt} \tag{8}$$

$$\psi_{s\alpha} = L_s \frac{i_\alpha}{\sqrt{3}} + \psi_m \cos(\theta_e) \tag{9}$$

$$\psi_{s\beta} = L_s \frac{i_\beta}{\sqrt{3}} + \psi_m \sin(\theta_e) \tag{10}$$

$$T_e = \frac{\sqrt{3}}{2} p(\psi_{s\alpha} i_\beta - \psi_{s\beta} i_\alpha) \tag{11}$$

where $i_{\alpha,\beta}$, $v_{\alpha,\beta}$, $\psi_{s\alpha,\beta}$ are respectively the transformed (*αβ*) currents, voltages, and stator fluxes. It is worth noting that the proposed mathematical model in the (*αβ*) reference frame for SPM BLAC machine under SOF shown in (7)-(11) is achieved by simply modifying the conventional Clarke transformation for the two remaining stator phase currents in the post-fault operation region. The magnitude and angular position of the stator flux linkage vector, $|\psi_s|$ and θ_{ψ_s}, are given by

$$|\psi_s| = \sqrt{\psi_{s\alpha}^2 + \psi_{s\beta}^2} \,; \qquad \theta_{\psi_s} = \arctan\left(\frac{\psi_{s\beta}}{\psi_{s\alpha}}\right) \tag{12}$$

It is also noted that when the open phase is phase *b* or *c*, the modified (*αβ*) mathematical model presented in (7)-(11) needs

to be rotated by either $2\pi/3$ (rad/s) or $4\pi/3$ (rad/s) using relevant transformation matrices [8].

3. Direct torque control of an ELES inverter SPM BLAC drive having SOF

In a DTC-based drive system, the electromagnetic torque and the stator flux linkage magnitude are simultaneously controlled through a predefined optimum switching table to achieve high performance operation [3], [15]. For an ELES inverter, there are eight available switching states associated with three inverter legs (*N,B,C*) [Fig. 1(b)]. Conventionally, voltage values of the two remaining stator phases can be calculated from these switching states, $S_{N,B,C}$, together with measurement of the DC link voltage, V_{dc} [3], [15].

$$v_{bn} = V_{dc}(S_B - S_N);\ v_{cn} = V_{dc}(S_C - S_N) \tag{13}$$

The status of the switching state in (13) is described as "1" when its equivalent stator terminal is connected to DC link voltage rail and "0" if it is linked to zero voltage rail. Substituting (13) into (6) together with arbitrarily setting the value of the voltage induced in the stator open phase winding as zero due to its non-torque producing characteristic, the active voltage vectors associated with the torque production in the ($\alpha\beta$) reference frame, $v_{\alpha-active}$ and $v_{\beta-active}$, can be calculated by

$$v_{\alpha-active} = V_{dc}\frac{2S_N - S_B - S_C}{3};\ v_{\beta-active} = V_{dc}\frac{S_B - S_C}{\sqrt{3}} \tag{14}$$

Table 1 Active voltage vectors of ELES inverter [10]

$v_{i=0\div7}$	$S_{N,B,C}$	v_{bn}	v_{cn}	$v_{\alpha-active}$	$v_{\beta-active}$
0	000	0	0	0	0
1	100	$-V_{dc}$	$-V_{dc}$	$2V_{dc}/3$	0
2	110	0	$-V_{dc}$	$V_{dc}/3$	$V_{dc}/\sqrt{3}$
3	010	V_{dc}	0	$-V_{dc}/3$	$V_{dc}/\sqrt{3}$
4	011	V_{dc}	V_{dc}	$-2V_{dc}/3$	0
5	001	0	V_{dc}	$-V_{dc}/3$	$-V_{dc}/\sqrt{3}$
6	101	$-V_{dc}$	0	$V_{dc}/3$	$-V_{dc}/\sqrt{3}$
7	111	0	0	0	0

Table 1 and Fig. 2(a) present active ($\alpha\beta$) voltage vectors of the ELES inverter derived from (14) [10]. Obviously, value of the active voltage space vector in the ELES inverter [Fig. 2(a)] is similar to that in the SSTP inverter [3], [15]. Therefore, a PM BLAC drive having SOF fed by an ELES inverter can be driven up to its rated speed.

In [16], the active voltage vectors in the ($\alpha\beta$) plane [Fig. 2(a)] were used to study DTC of a SPM BLAC drive with SOF fed by an ELES inverter. From this research, a modified switching table for DTC implementation, in which the stator flux ($\alpha\beta$) plane is divided into six equal sectors spaced 60 electrical degrees in the same fashion as that in the healthy case [3] was proposed [Fig. 2(b) and Table 2].

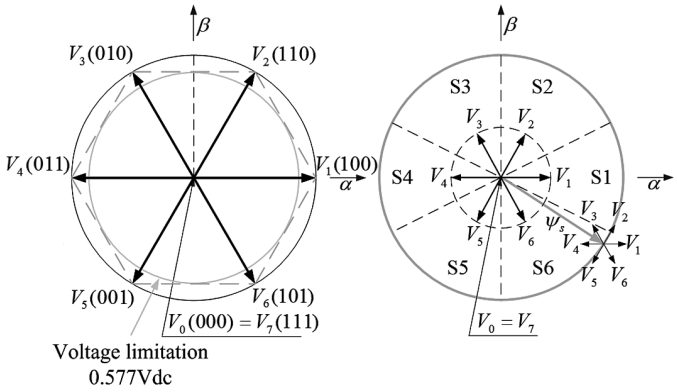

Fig. 2 *Active voltage vectors in the ($\alpha\beta$) plane of the ELES inverter*
a Diagram
b Control of stator flux linkage space vector in DTC-based ELES inverter utilizing active voltage vectors [16]

Table 2 Optimum switching table of DTC-based ELES inverter [16]

$d\lvert\psi_s\rvert$	dT_e	Sector					
		S1	S2	S3	S4	S5	S6
1	1	V_2	V_3	V_4	V_5	V_6	V_1
	0	V_7	V_0	V_7	V_0	V_7	V_0
	-1	V_6	V_1	V_2	V_3	V_4	V_5
0	1	V_3	V_4	V_5	V_6	V_1	V_2
	0	V_0	V_7	V_0	V_7	V_0	V_7
	-1	V_5	V_6	V_1	V_2	V_3	V_4

3.1 Current model-based DTC of an ELES inverter SPM BLAC drive under SOF

In a current model-based estimator, the stator flux linkage is estimated from the measurement of the stator phase currents, the information of the rotor position, and the PM flux linkage [15]. In the proposed current model-based estimator dedicated for the ELES inverter, the stator flux linkage components are estimated via (9) and (10). Then, the estimated values of the electromagnetic torque, the stator flux linkage magnitude, and the position information of the stator flux linkage space vector are respectively computed using (11) and (12). Subsequently, these estimated results are compared with their references via two hysteresis comparators, one is a two-state hysteresis controller for stator flux linkage magnitude control and the other is a three-state hysteresis controller for electromagnetic torque control. The outputs of these two comparators, $d\lvert\psi_s\rvert$ and dT_e, are defined as follows

$$d\lvert\psi_s\rvert = \begin{cases} 1 & \text{for } \lvert\psi_s^*\rvert - \lvert\psi_s\rvert > \dfrac{\Delta\psi_s}{2} \\ 0 & \text{for } \lvert\psi_s^*\rvert - \lvert\psi_s\rvert \le -\dfrac{\Delta\psi_s}{2} \end{cases} \tag{15}$$

$$dT_e = \begin{cases} 1 & \text{for } T_e^* - T_e > \dfrac{\Delta T_e}{2} \\ 0 & \text{for } \left|T_e^* - T_e\right| \le \dfrac{\Delta T_e}{2} \\ -1 & \text{for } T_e^* - T_e < -\dfrac{\Delta T_e}{2} \end{cases} \quad (16)$$

where ΔT_e is the torque hysteresis band, $\Delta\psi_s$ is the stator flux hysteresis band, * is the superscript indicating the reference values, respectively. These two control states, together with the stator flux linkage position information defined in equivalent sector [Fig. 2(b)] are used as the input of the optimum switching table (Table 2) to determine the inverter gate drive signals. The block diagram of the proposed current model-based DTC ELES inverter SPM BLAC drive under SOF and the proposed current model-based estimator is illustrated in Fig. 3(a) and Fig. 3(b) where ω_e and ω_e^* are the electrical rotor speed and its reference value, respectively. It is worth noting that implementation of the proposed current model-based stator flux estimation scheme requires the information of stator inductance, PM flux linkage, phase currents, and rotor position as that in the healthy case [15].

3.2 Voltage model-based DTC of an ELES inverter SPM BLAC drive under SOF

In a voltage model-based estimator, the stator flux linkage is estimated from the measurements of the stator phase currents and the calculation of the stator phase voltages [3], [15]. In the proposed voltage model-based estimator dedicated for the ELES scheme, the stator flux linkage components are estimated via (7) and (8). However, as aforementioned in Section 2, to compute the ($\alpha\beta$) voltages, value of the voltage induced in the stator open phase winding (phase *a* in this study) is necessarily required. For simplicity, this induced voltage can be computed from the voltage and current values of the two remaining stator phases as explained below.

Assuming that the SOF in its occurrence does not cause any damage to the original stator winding structure, due to the symmetry of the stator winding, the balanced conditions of the stator flux linkage components established by the permanent magnet, $\psi_{ra,rb,rc}$, and the stator phase back-EMFs, $e_{a,b,c}$, are still satisfied in the post-fault operation region. Thus

$$\psi_{ra} + \psi_{rb} + \psi_{rc} = 0\,;\; e_a + e_b + e_c = 0 \quad (17)$$

By substituting (17) into (1) to give

$$v_{an} = R_s(i_b + i_c) + L_{ls}\frac{d(i_b + i_c)}{dt} - v_{bn} - v_{cn} \quad (18)$$

Equation (18) is used to estimate value of the voltage induced in the stator open phase winding in the post-fault

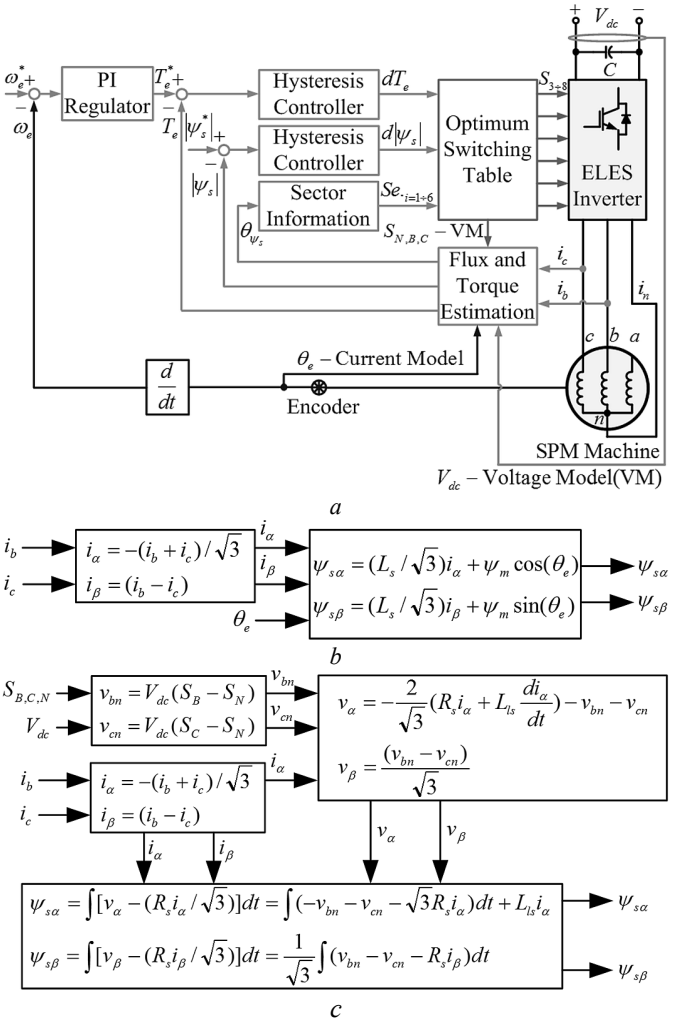

Fig. 3 *DTC scheme of ELES inverter SPM BLAC drive under SOF*
a DTC diagram
b Block diagram of proposed current model-based estimator
c Block diagram of proposed voltage model-based estimator

operation region. Substituting (18) into (6) and solving it by using (5) to give

$$v_\alpha = -\frac{2}{\sqrt{3}}\left(R_s i_\alpha + L_{ls}\frac{di_\alpha}{dt}\right) - v_{bn} - v_{cn} \quad (19)$$

$$v_\beta = \frac{(v_{bn} - v_{cn})}{\sqrt{3}} \quad (20)$$

Substituting (19), (20) into (7) and (8) and solving to yield

$$\psi_{s\alpha} = \int\left(v_\alpha - R_s\frac{i_\alpha}{\sqrt{3}}\right)dt = \int\left(-v_{bn} - v_{cn} - \sqrt{3}R_s i_\alpha\right)dt + L_{ls}i_\alpha \quad (21)$$

$$\psi_{s\beta} = \int\left(v_\beta - R_s\frac{i_\beta}{\sqrt{3}}\right)dt = \frac{1}{\sqrt{3}}\int\left(v_{bn} - v_{cn} - R_s i_\beta\right)dt \quad (22)$$

The block diagram representation of the proposed voltage model-based DTC ELES inverter SPM BLAC drive under SOF is the same as that of the proposed current model-based DTC [Fig. 3(a)] where information of the rotor position and

stator phase currents is utilized in the proposed current model-based estimator whereas knowledge of the switching states, DC link voltage, and stator phase currents is employed for the proposed voltage model-based scheme. The proposed voltage model-based stator flux estimator is illustrated in Fig. 3(c). It is worth noting that implementation of the proposed voltage model-based stator flux estimation scheme requires the information of stator resistance, phase voltages, and phase currents as that in the healthy case [15] together with the leakage inductance of which value can be obtained using the measurement technique described in [19]. The most advantage of the proposed voltage model-based stator flux estimation scheme is its implementation does not rely on the rotor position information, Fig. 3(c). In practice, a first-order low-pass filter (LPF) is utilized instead of the pure integrator to avoid integration drift problems [20]. However, machine drive with first-order LPF as stator flux estimator can only maintain a limited speed range (typically 1:10) [20] due to the magnitude and phase errors associated with the employed first-order LPF. Therefore, some improved techniques should be considered when a higher operating speed range is required for machine drive with voltage model-based stator flux estimator [20], [21], and [22].

In the next section, measured results of the proposed voltage model-based and current model-based stator flux estimators derived from the tested ELES inverter SPM BLAC drive with SOF under both ITC [14] and DTC will be presented to validate the suggested stator flux estimation schemes.

4. Imbalanced IVD issue with voltage model-based stator flux estimation with ELES inverter and proposed improvement

4.1 Problems of IVD imbalance with voltage model-based stator flux estimation with ELES Inverter

In practice, the stator phase voltage values, for simplicity, are conventionally computed from the inverter switching states and the DC link voltage measurement [3] in which the IVD is neglected [see (13) and Fig. 3(c)]. In [15], it was demonstrated that the IVD is balanced in three stator phases for a SSTP inverter SPM BLAC drive. However, in an ELES inverter SPM BLAC drive with SOF, the α- and β-IVD components are imbalanced as explained below.

Basically, the IVD of one inverter leg (*N,B,C*) of the ELES scheme [Fig. 1(b)] presented by a switching device or a free-wheeling diode, v_{IVD}, can be represented by a forward voltage drop, v_f, connected in series with an on-state resistance voltage drop, $R_{on}i$ [23].

$$v_{IVD} = v_f + R_{on}i \tag{23}$$

Substituting (23) into (1) leads to

$$v_{bn} = R_s i_b + R_{on}(i_b + i_n) + v_{fb} + v_{fn} + \frac{d\psi_{sb}}{dt} \tag{24}$$

$$v_{cn} = R_s i_c + R_{on}(i_c + i_n) + v_{fc} + v_{fn} + \frac{d\psi_{sc}}{dt} \tag{25}$$

$$i_n = i_b + i_c \tag{26}$$

where i_n is the neutral current. Substituting (24), (25), (26) into (21), (22) and solving leads to

$$\psi_{s\alpha} = \int (v_\alpha - R_s \frac{i_\alpha}{\sqrt{3}} - 3\sqrt{3}R_{on}i_\alpha + v_{f\alpha})dt \tag{27}$$

$$\psi_{s\beta} = \int (v_\beta - R_s \frac{i_\beta}{\sqrt{3}} - \frac{R_{on}}{\sqrt{3}}i_\beta + v_{f\beta})dt \tag{28}$$

$$v_{f\alpha} = v_{fb} + v_{fc} + 2v_{fn}\,; \quad v_{f\beta} = -\frac{v_{fb} - v_{fc}}{\sqrt{3}} \tag{29}$$

where $v_{f\alpha}$ and $v_{f\beta}$ are the transformed ($\alpha\beta$) inverter forward voltage drop components. As can be seen from (27) and (28), the on-state resistance voltage drop α-component of the ELES scheme is higher than that of the β-component. In addition, forward voltage drop of an inverter leg depends on both its instantaneous switching state and current direction [23]. This voltage drop varies between the values of forward voltage drop of IGBT, V_{CE}, and free-wheeling power diode, V_d, as shown in Table 3.

Table 3 On-state forward voltage drop on one inverter leg [23]

Switching states	Current direction	v_f
0	+	V_d
	–	$-V_{CE}$
1	+	V_{CE}
	–	$-V_d$

Table 4 Parameters of prototype inverter drive (IRAMY20UP60B)

$V_{CE} = V_d = V_F$	0.9V
R_{on}	0.075Ω

For simplicity, assuming that forward voltage of both switching device and free-wheeling power diode have the same value, Table 4, and therefore the forward voltage drop of an inverter leg depends only on its current direction. Thus, (29) can be simplified to give

$$v_{f\alpha} = V_F[sign(i_b) + sign(i_c) + 2sign(i_n)] \tag{30}$$

$$v_{f\beta} = -\frac{V_F[sign(i_b) - sign(i_c)]}{\sqrt{3}} \tag{31}$$

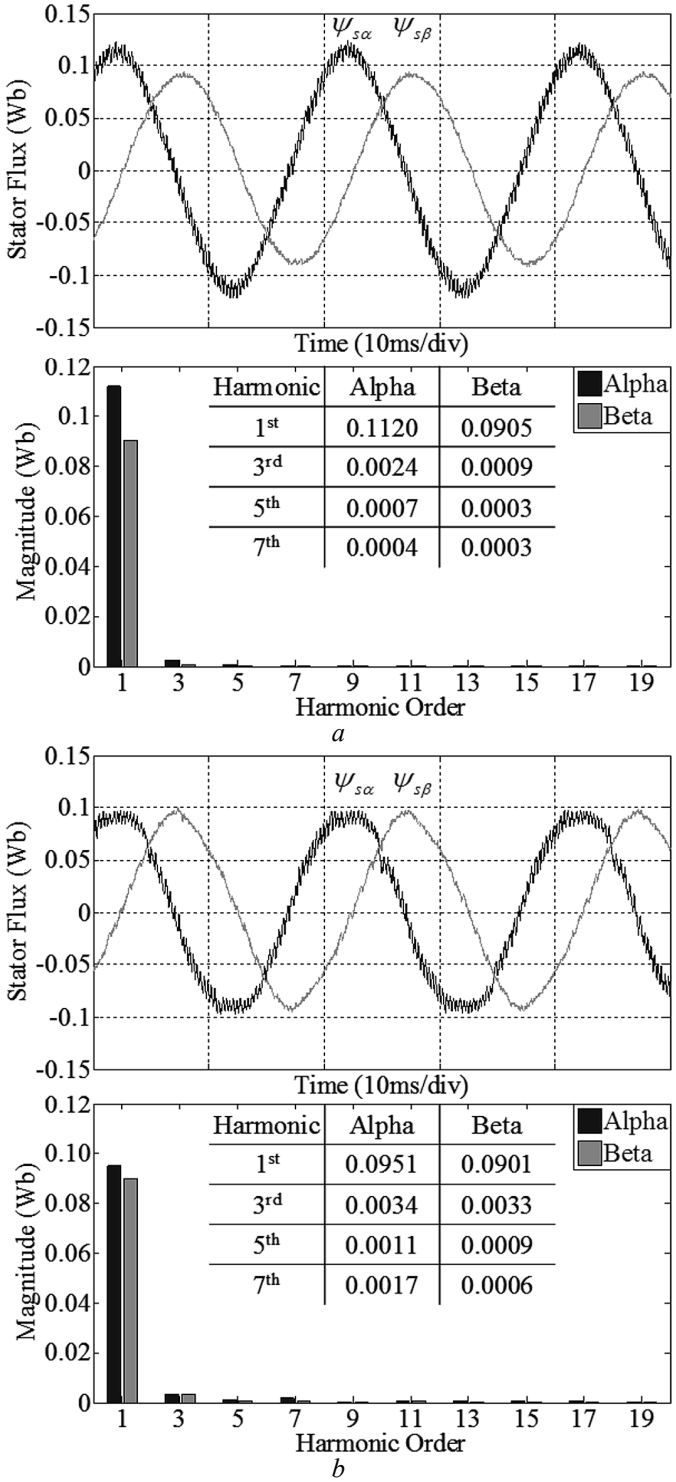

Harmonic	Alpha	Beta
1st	0.1120	0.0905
3rd	0.0024	0.0009
5th	0.0007	0.0003
7th	0.0004	0.0003

Harmonic	Alpha	Beta
1st	0.0951	0.0901
3rd	0.0034	0.0033
5th	0.0011	0.0009
7th	0.0017	0.0006

Fig. 4 *Experimental results from proposed voltage model-based stator flux estimator for ELES scheme at 3000rpm without compensation for IVD, full load applied (0.3Nm)*
a Under ITC [14]
b Under DTC

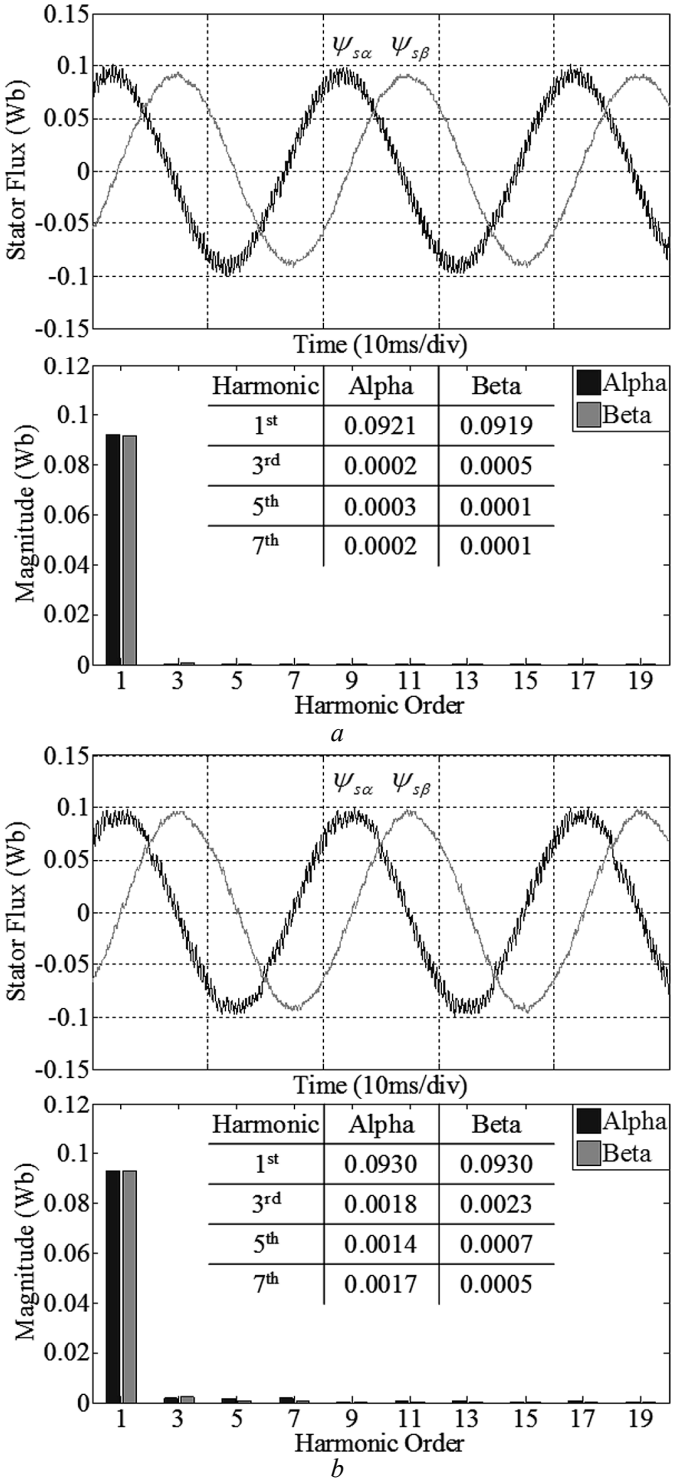

Harmonic	Alpha	Beta
1st	0.0921	0.0919
3rd	0.0002	0.0005
5th	0.0003	0.0001
7th	0.0002	0.0001

Harmonic	Alpha	Beta
1st	0.0930	0.0930
3rd	0.0018	0.0023
5th	0.0014	0.0007
7th	0.0017	0.0005

Fig. 5 *Experimental results from proposed voltage model-based stator flux estimator for ELES scheme at 3000rpm incorporating proposed IVD compensation scheme, full load applied (0.3Nm)*
a Under ITC [14]
b Under DTC

By adopting (30) and (31), the forward voltage drop components of the ELES scheme can be derived as shown in Table 5. Obviously, the value of the inverter forward voltage drop α-component is higher than that of the β-component.

By combination the impacts of both the inverter on-state resistance and forward voltage drop analyses, it can be proven that without accounting for these effects, magnitude of the estimated stator flux linkage α-component derived from the proposed voltage model-based estimator [Fig. 3(c)] is higher than that of the β-component, and therefore, the current waveforms under the proposed voltage model-based DTC ELES inverter SPM BLAC drive with SOF become seriously

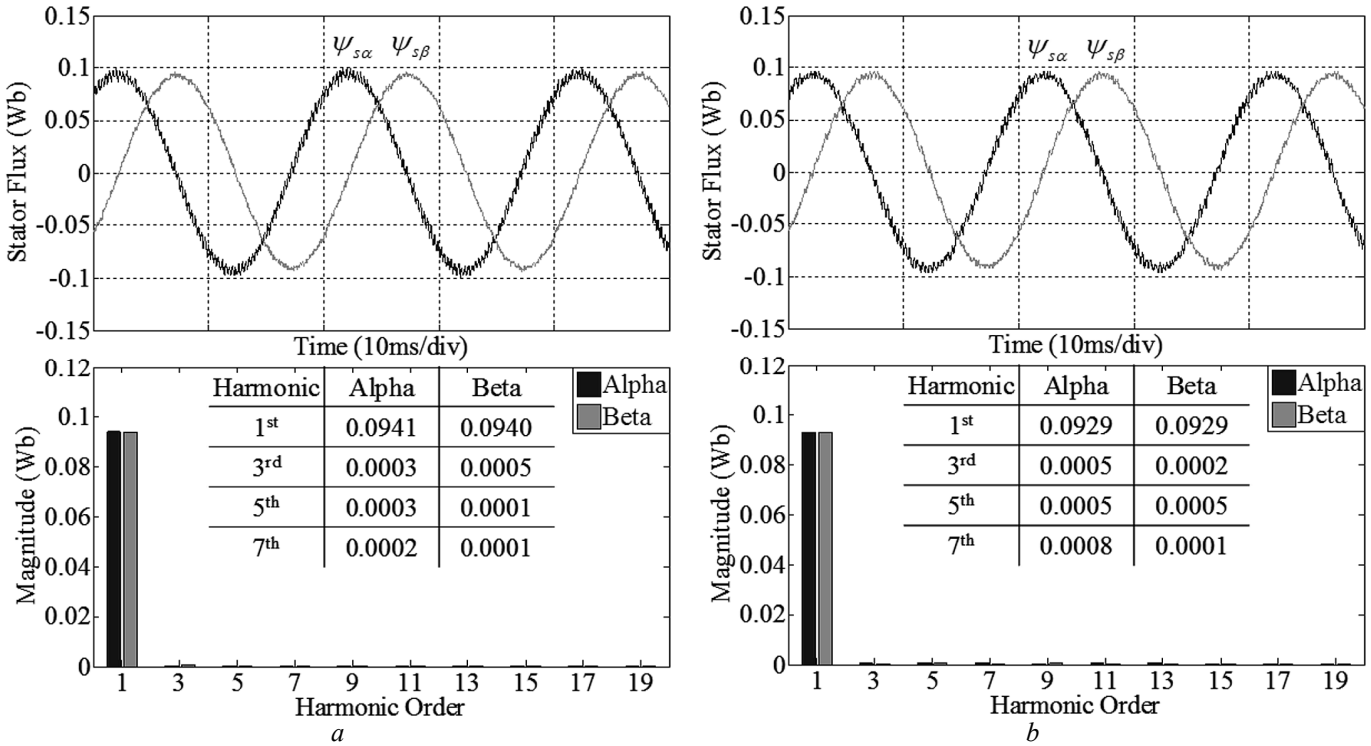

Harmonic	Alpha	Beta
1st	0.0941	0.0940
3rd	0.0003	0.0005
5th	0.0003	0.0001
7th	0.0002	0.0001

Harmonic	Alpha	Beta
1st	0.0929	0.0929
3rd	0.0005	0.0002
5th	0.0005	0.0005
7th	0.0008	0.0001

Fig. 6 *Experimental results from proposed current model-based stator flux estimator for ELES scheme at 3000rpm, full load applied (0.3Nm)*
a Under ITC [14]
b Under DTC

distorted due to incorrect decision on choosing optimum switching states of the drive system (see Figs. 9 and 11(a) in Section 5, similar phenomenon can be found in [15] and [16]).

Table 5 On-state forward voltage drop vectors in an ELES inverter

$sign(i_b)$	$sign(i_c)$	$sign(i_n)$	$v_{f\alpha}$	$v_{f\beta}$
–	–	–	$-4V_F$	0
–	–	+	0	0
–	+	–	$-2V_F$	$2V_F/\sqrt{3}$
–	+	+	$2V_F$	$2V_F/\sqrt{3}$
+	–	–	$-2V_F$	$-2V_F/\sqrt{3}$
+	–	+	$2V_F$	$-2V_F/\sqrt{3}$
+	+	–	0	0
+	+	+	$4V_F$	0

Since the peaks of the stator flux linkage α- and β-components are directly controlled and forced to be equal together under DTC [Fig. 3(a)], to demonstrate the proposed stator flux estimation schemes and emphasize the aforementioned imbalanced issue, measured results of estimated stator flux linkage of the tested SPM BLAC drive having SOF fed by an ELES inverter under both ITC [14] and DTC using the proposed voltage model-based estimator without IVD compensation are presented in Fig. 4. Obviously, the fundamental harmonic of the stator flux linkage α-component under ITC is much higher than that of the β-component [Fig. 4(a)]. However, the fundamental harmonics of the stator flux linkage α- and β-components under DTC are still significantly different [Fig. 4(b)]. It is worth noting that the α-stator flux linkage component under the proposed voltage model-based estimator contains switching harmonics due to the component $L_{ls}i_\alpha$ shown in (21).

4.2 Compensation of IVD in voltage model-based stator flux estimation with ELES inverter

In [15], the effects of imbalanced IVD on a four-switch three-phase inverter was reported and compensated by including the inverter on-state resistance and inverter forward voltage drops into the voltage equations. The same technique is adopted in this paper to compensate for the unbalanced IVD in the ELES scheme by utilizing (27), (28), Table 4, and Table 5. Fig. 5 presents measured results of the estimated stator flux linkage of the tested ELES drive under both ITC [14] and DTC derived from the proposed voltage model-based stator flux estimator incorporating the IVD compensation scheme. Obviously, the imbalance between the estimated stator flux linkage α- and β-components is considerably reduced.

On the other hand, since the proposed current model-based stator flux estimator does not require voltage calculation [Fig. 3(b)], measured results of the tested ELES drive under both ITC [14] and DTC in Fig. 6 show that the proposed current model-based estimator are not affected by the aforementioned imbalanced IVD issue. It is worth noting that measured results of the estimated stator flux linkage $\alpha\beta$-components respectively shown in Figs. 5 and 6 experimentally validate the proposed voltage model-based and current model-based

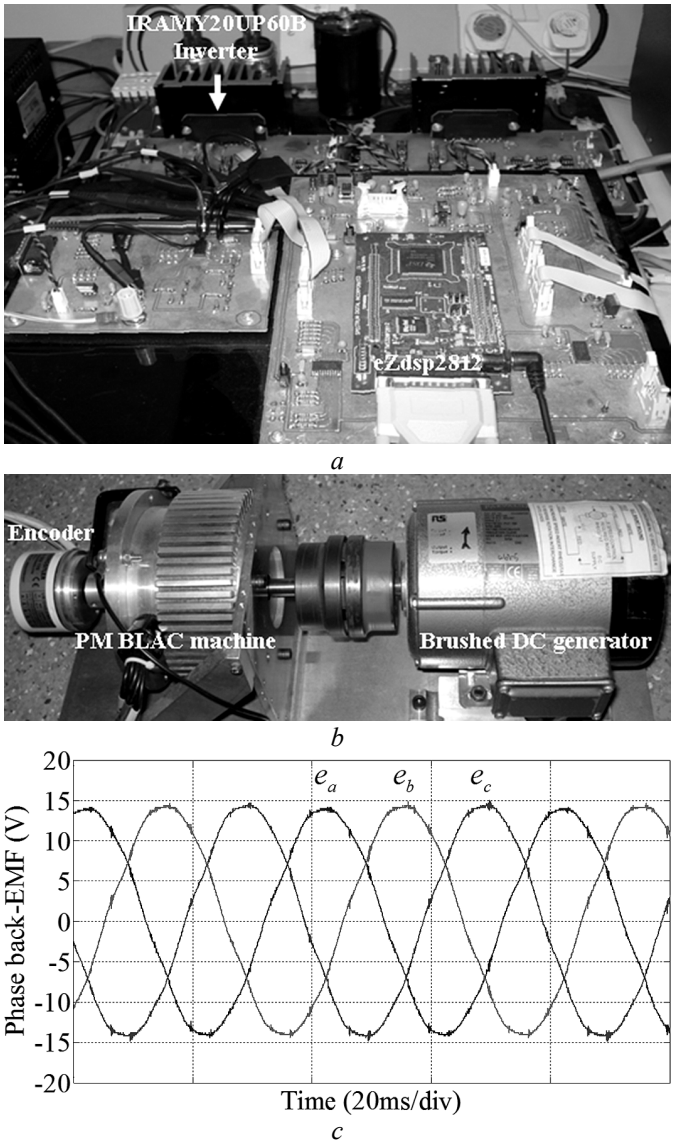

Fig. 7 Experimental hardware setup
a Inverter and DSP control platform
b SPM BLAC machine couple to brushed DC generator
c Measured back-EMF waveforms of SPM BLAC machine at 1500rpm

stator flux estimation schemes for the ELES inverter SPM BLAC drive having SOF under both ITC [14] and DTC.

5. Experimental results

In this section the measured results of DTC performance of the tested SPM BLAC machine with SOF fed by an ELES inverter is presented. The drive system is controlled by a 32-bit fixed-point TSM320-F2812 DSP and further details can be found in [15]. It has an inner loop sample time of 50μs for torque and flux control and the outer speed control loop is set to 10 times slower. For simplicity, $\Delta\psi_s$ is set as zero and ΔT_e is chosen as 2% of the rated torque. The stator flux linkage reference is set to peak value of the PM flux-linkage (92.8mWb). Pictures of the experimental setup are shown in Fig. 7. The employed machine has sinusoidal back-EMFs [Fig. 7(c)] with neutral connection and its equivalent circuit parameters together with ratings are provided in Table 6. A brushed DC generator is coupled to the tested SPM BLAC machine to deliver load torque. An incremental encoder (Hengstler RI58-O/2000AS.41RB) with 2000 pulses per revolution [Fig. 7(b)] is employed to provide the speed information for the PI speed controller of the proposed DTC-based ELES schemes under the speed control mode [Figs. 3(a)] and the rotor position information for the proposed current model-based stator flux estimator, Fig. 3(b). For the proposed voltage model-based stator flux estimator [Fig. 3(c)], the phase voltages are computed from the measured DC link voltage and the switching states of the inverter and a first-order LPF with a cut-off frequency of 5(rad/s) is utilized instead of a pure integrator to avoid integration drift problems [20]. For simplicity, only the steady state of the post-fault operating mode is considered. To demonstrate the performance of the proposed modified mathematical model, operation of the tested SPM BLAC machine driven by a SSTP inverter in the healthy case [15] is shown in Fig. 8.

Table 6 Parameters of tested SPM BLAC machine

Phase resistance	0.466 Ω
Dq-axis inductance	3.19 mH
Rotor magnetic flux	92.8 mWb
Number of pole pairs	1
DC bus voltage	70 V
Rated speed	3000 rpm
Rated torque	0.3 Nm
Rated current healthy/post-fault case	2.2/ 2.2$\sqrt{3}$ A

Table 7 Fundamental current values under various control modes

Healthy operating mode						
Model	Current-based			Voltage-based		
Phase	*a*	*b*	*c*	*a*	*b*	*c*
	2.32	2.28	2.30	2.20	2.24	2.28
Post-fault operating mode						
Model	Current-based		Voltage-based			
			None compensation		With compensation	
Phase	*b*	*c*	*b*	*c*	*b*	*c*
	3.80	3.85	4.66	3.60	3.85	3.78

In Fig. 9(a), simulation investigation of the proposed voltage model-based DTC ELES inverter SPM BLAC drive under SOF using MATLAB/SIMULINK is presented. It is worth noting that a single sampling time delay was employed in the simulation study to imitate the delaying time in the real drive system [16]. Obviously, when the non-ideal switching devices (Table 4) are employed in the simulation model, the current waveforms become seriously distorted. The simulated results presented in Fig. 9(a) match well with the measured results obtained from the tested voltage model-based DTC ELES inverter [Fig. 9(b)]. Also from Fig. 9, a higher estimated torque value than the real shaft torque (0.3Nm) will be seen by the drive system if the inverter non-idealizes are neglected [15] and therefore, a higher demanded current value

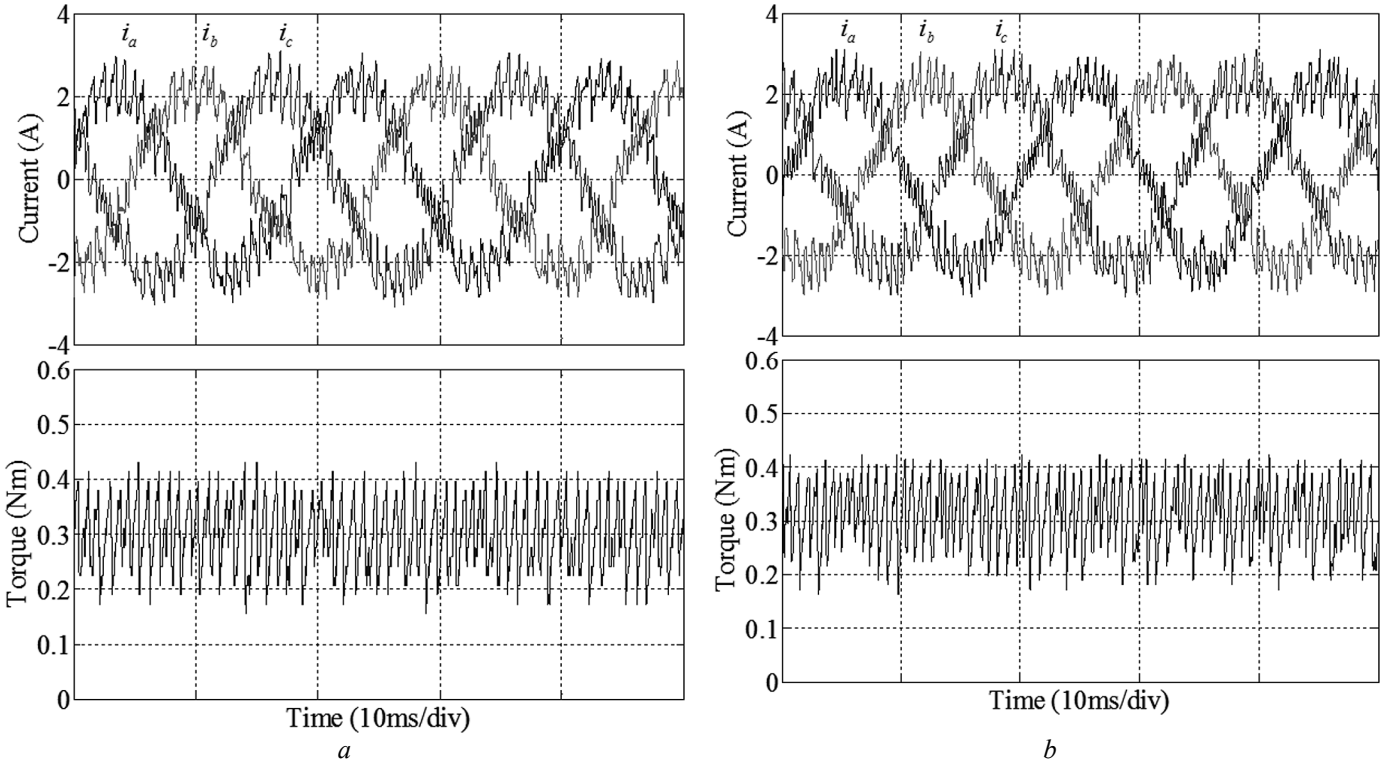

Fig. 8 *Measured results of SSTP inverter at 3000rpm, full load applied (0.3Nm)*
a Voltage model-based DTC
b Current model-based DTC

than its real necessary ($2.2\sqrt{3}$ A) is required by the controller (Table 7) to satisfy this incorrectly estimated torque value.

Comparison between Fig. 9 and Fig. 10(a) clearly demonstrates the performance enhancement of the proposed voltage model-based DTC ELES inverter incorporating the IVD compensation scheme with balanced sinusoidal phase current waveforms, reduction of incorrectly estimated torque value and therefore, decrease of phase current magnitude, Table 7. On the other hand, sinusoidal current waveforms shown in Fig. 10(b) clearly prove that performance of the proposed current model-based DTC ELES scheme is not adversely affected by the aforementioned unbalanced IVD issue. Additionally, it is evident from Fig. 10 and Table 7 that without any current control technique, the post-fault operating conditions required for the two remaining stator phase currents under the ELES scheme [9]-[14] are completely satisfied with the stator phase current waveforms are 60 electrical degrees phase shift together and their magnitudes increase $\sqrt{3}$ times compared with the healthy case (Fig. 8 and Table 7). To demonstrate the effectiveness of the proposed voltage model-based DTC ELES scheme, measured results of the tested PM BLAC machine operating at 1500rpm are shown in Fig. 11.

6. Conclusion

In this paper, a modified mathematical model with novel current model-based and voltage model-based stator flux estimation schemes for fault-tolerant control of a DTC-based SPM BLAC drive under SOF has been presented and validated by both simulation and experimental results. It has been demonstrated that the proposed mathematical model can be achieved by simply modifying the conventional Clarke transformation for the two remaining stator phase currents in the post-fault operation region. Thus, it has been proven that for accurately elaborating the modified mathematical model, the voltage induced in the stator open phase winding and its relevant stator flux linkage should be taken into account although they do not contribute to torque production in the post-fault operating mode.

It has been also demonstrated that reconfiguration from the SSTP to the ELES schemes for fault-tolerant control purpose results in an imbalance between the $\alpha\beta$-IVD components and therefore conventionally neglecting the IVD in the proposed voltage model-based estimator does lead to significant magnitude imbalance between the estimated stator flux linkage components. Hence, current waveforms under the proposed voltage model-based DTC become seriously distorted due to incorrect decision on choosing optimum switching states of the drive system. To solve this problem, a compensation scheme has been suggested and experimentally validated. Additionally, it has been proven that performance of the proposed current model-based DTC is not adversely affected by this imbalanced issue.

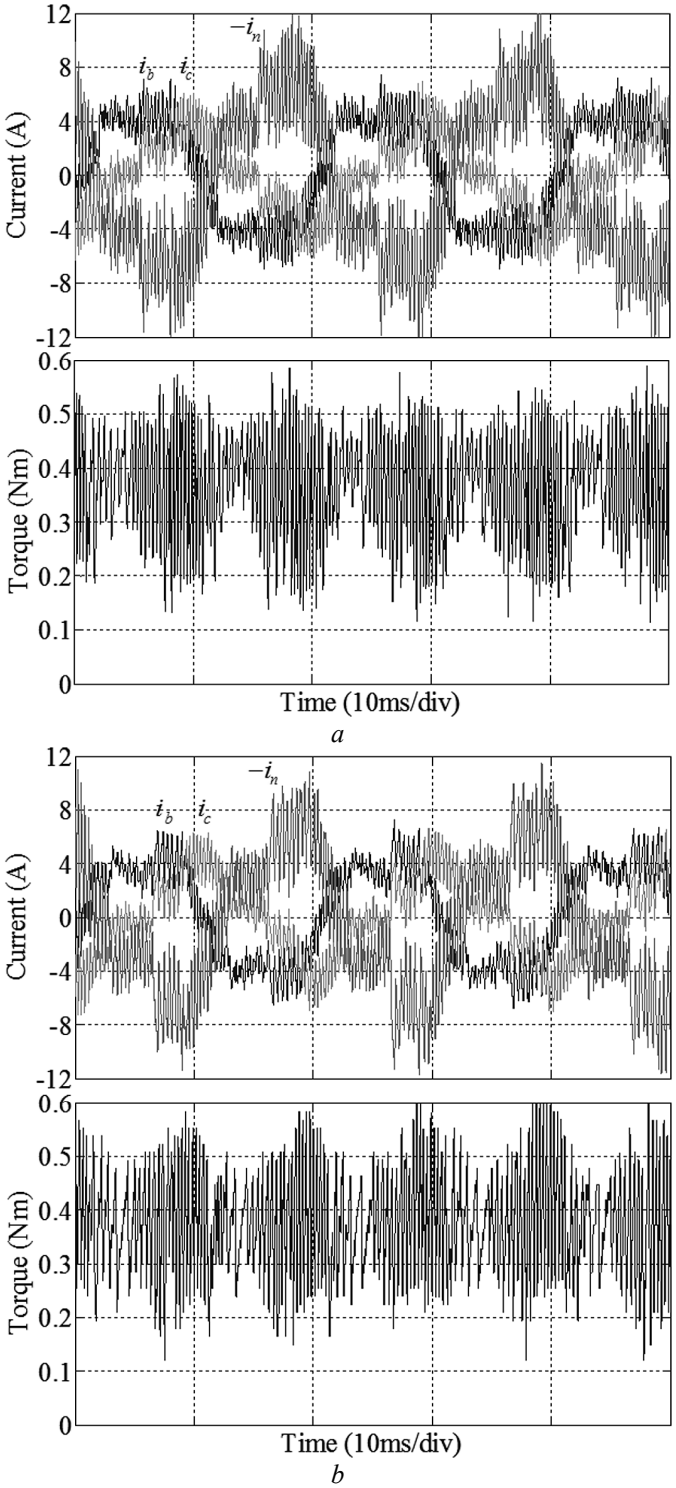

Fig. 9 *Simulated and measured results of proposed voltage model-based DTC ELES inverter at 3000rpm without compensation for IVD, full load applied (0.3Nm)*
a Simulated results
b Measured results

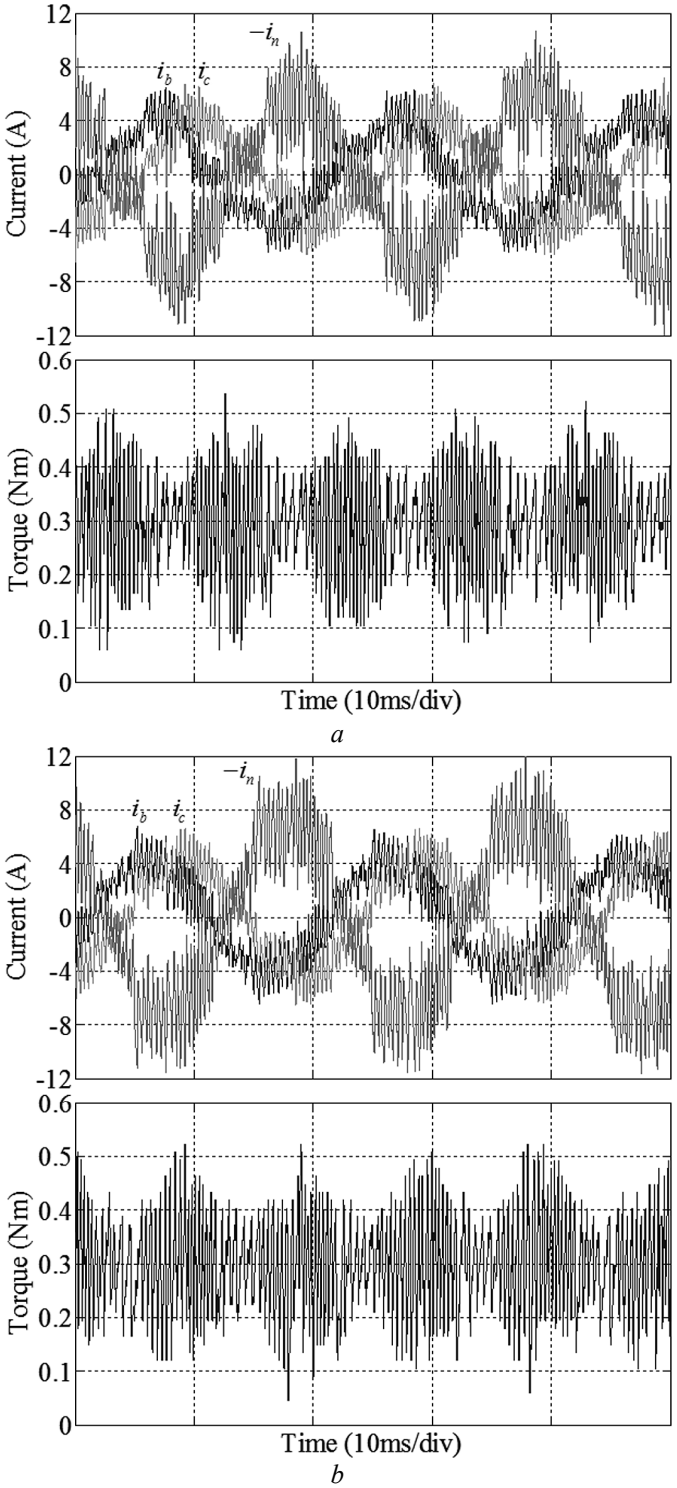

Fig. 10 *Measured results of ELES inverter at 3000rpm, full load applied (0.3Nm)*
a Proposed voltage model-based DTC incorporating compensation for IVD
b Proposed current model-based DTC

Although the paper is only focused on 3-phase SPM BLAC machine, the proposed technique is equally applicable to IPM BLAC machines. The relevant research such as sensorless control of PM BLAC drive under SOF based on the proposed voltage model-based stator flux estimation scheme is being further investigated and will be reported in another paper.

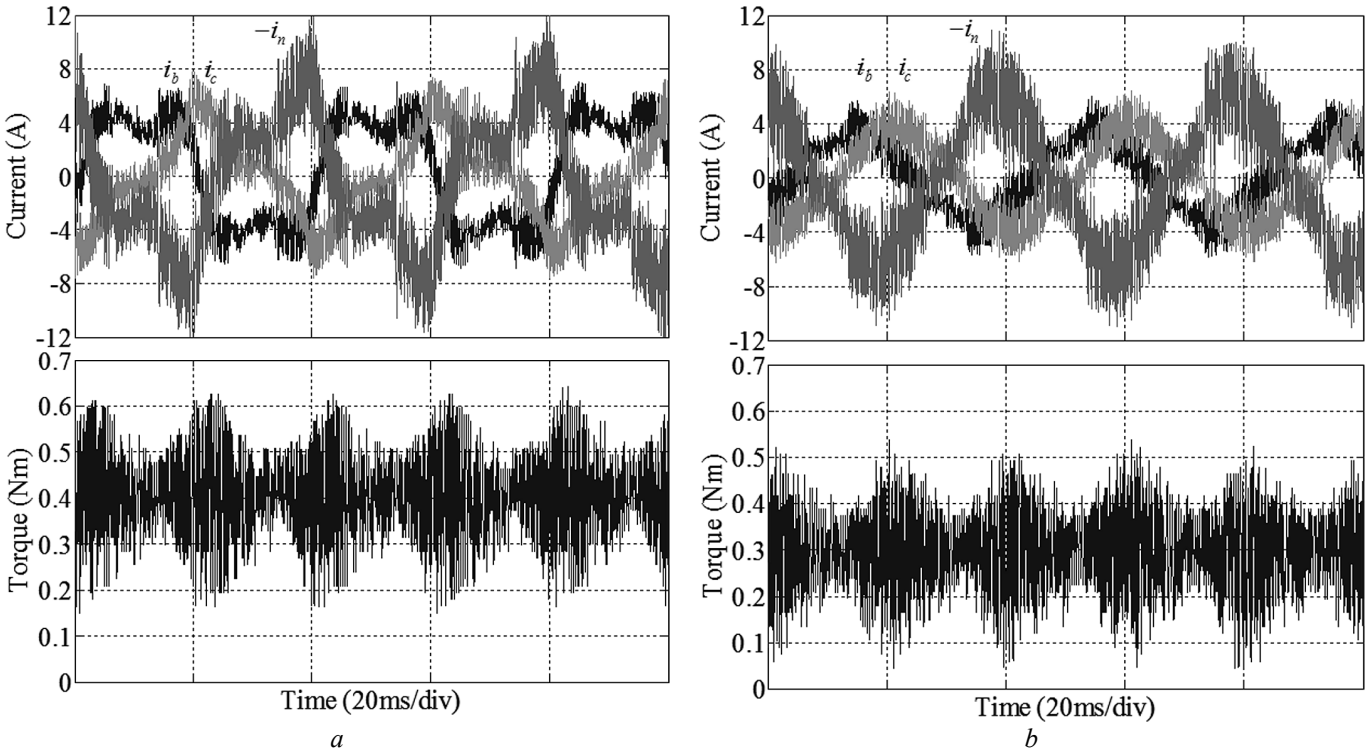

Fig. 11 *Measured results of proposed voltage model-based ELES inverter at 1500rpm, full load applied (0.3Nm)*
a Without compensation for IVD
b Incorporating compensation for IVD

7. Appendix

Assuming phase *a* is the open phase and the two remaining stator phase current waveforms satisfy the post-fault operating conditions with 60 electrical degrees phase shift together and their magnitudes increase $\sqrt{3}$ times compared with the healthy case [10].

$$i_b = \sqrt{3} I_m \sin\left(\omega_e t - \frac{2\pi}{3} - \frac{\pi}{6}\right) \quad \text{(A1)}$$

$$i_c = \sqrt{3} I_m \sin\left(\omega_e t - \frac{4\pi}{3} + \frac{\pi}{6}\right) \quad \text{(A2)}$$

where I_m is the phase current magnitude in the healthy operating mode.

Substituting (A1) and (A2) into (5) and solving leads to

$$i_\alpha = \frac{\sqrt{3}}{2} K \sqrt{3} I_m \sin(\omega_e t) \quad \text{(A3)}$$

$$i_\beta = -\frac{\sqrt{3}}{2} K \sqrt{3} I_m \cos(\omega_e t) \quad \text{(A4)}$$

From (A3) and (A4), it can be concluded that to achieve magnitude invariant conversion, value of the *K* factor must be chosen as $2/\sqrt{3}$.

8. References

1 Pillay, P., Krishnan, R.: 'Modelling, simulation, and analysis of permanent-magnet motor drives, part I: the permanent-magnet synchronous motor drive'. *IEEE Trans. Ind. Appl.*, 1989, **25**, pp. 265-273

2 Wipasuramonton, P., Zhu, Z.Q., Howe, D.: 'Improved current-regulated delta modulator for reducing switching frequency and low-frequency current error in permanent magnet brushless AC drives'. *IEEE Trans. Power Electron.*, 2005, **20**, pp. 75-484

3 Zhong, L., Rahman, M.F., Hu, W.Y., Lim, K.W.: 'Analysis of direct torque control in permanent magnet synchronous motor drives'. *IEEE Trans. Power Electron.*, 1997, **12**, pp. 528-536

4 Fu, J.R., Lipo, T.: 'A strategy to isolate the switching device fault of a current regulated motor drive'. in Conf. Rec. IEEE−IAS Annu. Meeting, vol. 01, 1993, pp. 1015-1020

5 Liu, T.H., Fu, J.R., Lipo T.A.: 'A strategy for improving reliability of field-oriented controlled induction motor drives'. *IEEE Trans. Ind. Appl.*, 1993, **29**, pp. 910-918

6 Mendes, A.M.S., Cardoso, A.J.M.: 'Fault-tolerant operating strategies applied to three-phase induction-motor drives'. *IEEE Trans. Ind. Electron.*, 2006, **53**, pp. 1807-1817

7 Kim, J., Hong, J., Nam, K.: 'A current distortion compensation scheme for four-switch converters'. *IEEE Trans. Power Electrons.*, 2009, **24**, pp. 1032-1040

8 Correa, M.B.R., Jacobina, C.B., Silva, E.R.C., Lima, A.M.N.: 'An induction motor drive system with improved fault tolerance'. *IEEE Trans. Ind. Appl.*, 2001, **37**, pp. 873-879

9 Bolognani, S., Zordan, M., Zigliotto, M.: 'Experimental fault-tolerant control of a PMSM drive'. *IEEE Trans. Ind. Appl.*, 2000, **47**, pp. 1134-1141

10 Bianchi, N., Bolognani, S., Zigliotto, M., Zordan, M.: 'Innovative remedial strategies for inverter faults in IPM synchronous motor drives'. *IEEE Trans. Energy Convers.*, 2003, **18**, pp. 306-314

11 Khwan-on, S., Lillo, L.D., Empringham, L., Wheeler, P., Gerada C.: 'Fault-tolerant, matrix converter, permanent magnet synchronous motor drive for open-circuit failures'. *IET Elect. Power Appl.*, 2011, **5**, pp. 654-667

12 Khwan-on, S., Lillo, L.D., Empringham, L., Wheeler, P.: 'Fault-tolerant matrix converter motor drives with fault detection of open switch faults'. *IEEE Trans. Ind, Appl.*, 2012, **59**, pp. 257-268
13 Wallmark, O., Harnefors, L., Carlson, O., 'Control algorithms for a fault-tolerant PMSM drive'. *IEEE Trans. Ind. Appl.*, 2007, **4**, pp. 1973-1980
14 Hoang, K.D., Zhu, Z.Q., Foster, M.P., Stone, D.A.: 'Comparative study of current vector control performance of alternate fault tolerant inverter topologies for three-phase PM brushless AC machine with one phase open-circuit fault'. Proc. 5th IET Int. Conf. Power Electron. Machines and Drives (PEMD), Apr. 19-21, 2010, pp. Mo4.1.3
15 Hoang, K.D., Zhu, Z.Q., Foster, M.P.: 'Influence and compensation of inverter voltage drop in direct torque controlled four-switch three-phase PM brushless AC drives'. *IEEE Trans. Power Electron.*, 2011, **26**, pp. 2343-2357
16 Zhu, Z.Q., Utaikaifa, K., Hoang, K., Liu, Y., Howe, D.: 'Direct torque control of three-phase PM brushless AC motor with one phase open-circuit fault'. Proc. IEEE Int. Electric Machines and Drives Conf. (IEMDC), May 3-6, 2009, pp. 1408-1415
17 Mohammed, O.A., Liu, S., Liu, Z.: 'Physical modelling of PM synchronous motors for integrated coupling with machine drives'. *IEEE Trans. Magn.*, 2005, **41**, pp. 1628-1631
18 Krause, P.C., Wasynczuk, O., Sudhoff, S.D.: 'Analysis of electric machinery and drive systems'. (Wiley-IEEE Press, 2002, 2nd edn.)
19 Gorman, S.F., Chen, C., Cathey, J.J.: 'Determination of permanent magnet synchronous motor parameters for use in brushless DC motor analysis'. *IEEE Trans. Energy Convers.*, 1988, **3**, pp. 674-681
20 Hu, J., Wu, B.: 'New integration algorithms for estimating motor flux over a wide-speed range'. *IEEE Trans. Power Electron*., 1998**, 13**, pp. 969–977
21 Bose, K.B., Patel, R.N.: 'A programmable cascaded low-pass filter-based flux synthesis for a stator flux-oriented vector-controlled induction motor drive', *IEEE Trans. Ind. Electron.*, 1997, **44**, pp. 140-143
22 Rahman, M. F., Haque, M.E., Tang, L., Zhong, L.: 'Problem associated with the direct torque control of an interior permanent-magnet synchronous motor drive and their remedies'. *IEEE Trans. Power Electron.*, 2004, **51**, pp. 799-809
23 Mohan, N., Undeland, T.M., Robbins, W.P.: 'Power electronics-Converters, Applications and Design, (John Wiley & Sons Inc. 1995)